Neuron 49, 467–479, February 2, 2006 ©2006 Elsevier Inc. DOI 10.1016/j.neuron.2006.01.007

Dissociable Codes of Odor Quality and Odorant Structure in Human Piriform Cortex

Jay A. Gottfried,[1,2,*] Joel S. Winston,[2] and Raymond J. Dolan[2]
[1] Cognitive Neurology and Alzheimer's Disease Center
Department of Neurology
Northwestern University Feinberg School of Medicine
320 East Superior Street
Chicago, Illinois 60611
[2] Wellcome Department of Imaging Neuroscience
12 Queen Square
London WC1N 3BG
United Kingdom

Summary

The relationship between odorant structure and odor quality has been a focus of olfactory research for 100 years, although no systematic correlations are yet apparent. Animal studies suggest that topographical representations of odorant structure in olfactory bulb form the perceptual basis of odor quality. Whether central olfactory regions are similarly organized is unclear. Using an olfactory version of fMRI cross-adaptation, we measured neural responses in primary olfactory (piriform) cortex as subjects smelled pairs of odorants systematically differing in quality and molecular functional group (as one critical attribute of odorant structure). Our results indicate a double dissociation in piriform cortex, whereby posterior regions encode quality (but not structure) and anterior regions encode structure (but not quality). The presence of structure-based codes suggests fidelity of sensory information arising from olfactory bulb. In turn, quality-based codes are independent of any simple structural configuration, implying that synthetic mechanisms may underlie our experience of smell.

Introduction

Clarifying the relationship between odorant structure and odor function (quality) is arguably one of the more critical issues in olfactory neuroscience. Why does one volatile organic compound "smell" like chocolate, and another like cheese? How is odor quality encoded in the brain? There has been very little systematic research to address these questions. For nearly 100 years, investigators have devised numerous categorization schemes of odor quality (Henning, 1916; Moncrieff, 1967; Amoore, 1972), none of which has withstood scientific scrutiny (e.g., Macdonald, 1922; Wise et al., 2000).

Ever since the first multigene family of olfactory receptors was identified (Buck and Axel, 1991), much olfactory research has concentrated on the odorant response profiles of olfactory sensory neurons in the nasal epithelium and their projection sites in olfactory bulb (OB) glomeruli. Animal studies indicate that specific molecular determinants of an odorant, such as functional group and carbon-chain length, govern the receptive field properties in olfactory sensory neurons (Zhao et al., 1998; Araneda et al., 2000; Touhara et al., 2000) and the OB (Imamura et al., 1992; Johnson et al., 1998; Rubin and Katz, 1999; Malnic et al., 1999; Xu et al., 2003). Complementary behavioral studies demonstrate that odorants evoking similar electrophysiological patterns in rodent OB engender similar behavioral responses (Linster et al., 2001). These findings have led to the idea that odor-specific spatial maps in the OB may underpin odor perception and that neural representations of odor quality are reflected in ensemble OB activity encoding complex configurations of molecular features.

However, the above observations conflict with human psychophysical studies showing that structurally related odorants may smell different and that structurally unrelated odorants may smell alike (Polak, 1973; Cain and Polak, 1992), highlighting an unpredictable relationship between olfactory sensation and odor perception. Such findings raise the question of whether the neural analog of an odor percept is directly the product of structure-based ensembles. Indeed, it is often noted that the perception of an odor is a synthetic process—the smell of chocolate may contain dozens, if not hundreds, of volatile organic compounds (Counet et al., 2002), yet the olfactory system synthesizes this complex mixture seamlessly into a single odor percept. Recent psychophysical studies have highlighted the integrative nature of odor perception (Stevenson, 2001; Wilson and Stevenson, 2003). Within this framework, an olfactory percept is as much defined by a myriad of molecular determinants as by previously stored odor representations and ongoing sensory context (Wilson and Stevenson, 2003).

The primary olfactory (piriform) cortex is one candidate site where synthetic, experience-dependent coding of odor quality may occur. As the principal target of OB afferents, this region is critically involved in olfactory memory and learning (Schoenbaum and Eichenbaum, 1995; Kay and Freeman, 1998; Mouly et al., 2001). Moreover, its unique anatomical organization has provided an attractive framework for computational models of associative memory, leading to proposals that piriform cortex is a repository of olfactory memory traces (Haberly and Bower, 1989). Indeed, single-unit recordings suggest that neuronal activity in rodent piriform cortex reflects encoding of odor objects and that piriform receptive fields are shaped through experience (Wilson, 2003).

In the present study, we used functional magnetic resonance imaging (fMRI) techniques to determine whether human piriform cortex encodes information about perceptual or structural determinants of smell. As used here, the term "quality" denotes odor-object identity, i.e., the perceptual character of a smell emanating from an odorous object (in contrast to other odor qualities, such as intensity or valence). We scanned healthy subjects during an olfactory version of fMRI

*Correspondence: j-gottfried@northwestern.edu

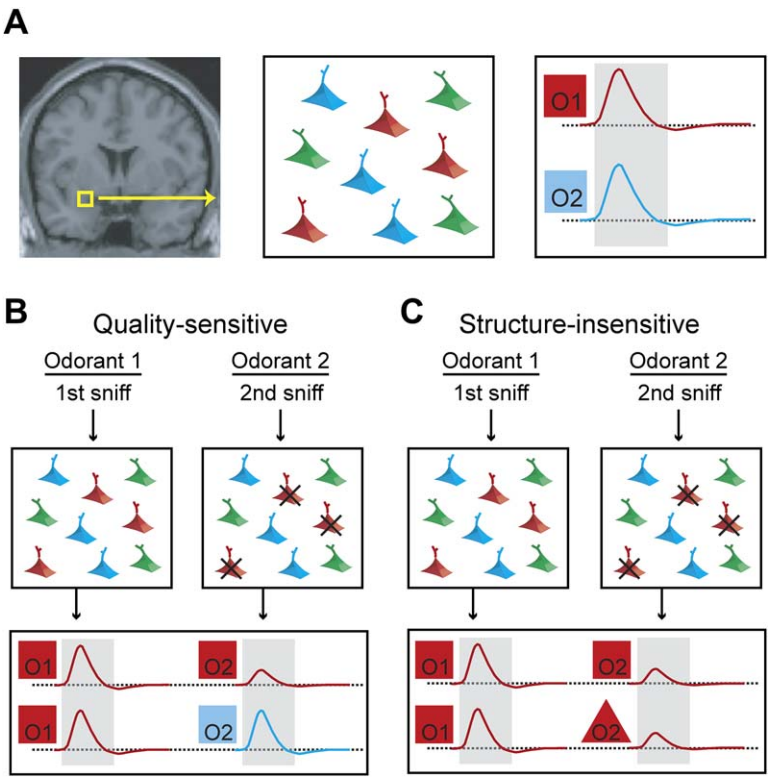

Figure 1. Schematic of Olfactory fMRI Cross-Adaptation

(A) This hypothetical piriform voxel (left) contains three spatially distributed neuronal populations (middle), each tuned to a different odor quality. Due to limited fMRI spatial resolution, presentation of one odorant (O1/red) evokes a hemodynamic response (right) indistinguishable from a qualitatively different odorant (O2/blue). Thus, in the absence of differential activity, one cannot demonstrate whether piriform cortex codes odor quality.

(B) In fMRI cross-adaptation, sequential presentation of two qualitatively similar odorants (O1/red, O2/red) causes adaptation in neurons encoding that particular quality (marked by "X"), leading to decreases in the evoked hemodynamic response, whereas qualitatively different odorant pairs (O1/red, O2/blue) evoke an undiminished (nonadapted) response. This differential pattern effectively unmasks piriform sensitivity to odor quality.

(C) In contrast, qualitatively similar pairs that differ in molecular functional group (O2/red square, O2/red triangle) evoke equivalent cross-adapting responses, indicating that this hypothetical voxel is insensitive (invariant) to this feature.

cross-adaptation in which odor quality and odorant structure were independently manipulated. Our design was modeled on previous experiments that used neuronal "repetition suppression" (Baylis and Rolls, 1987; Miller et al., 1991) or "fMRI adaptation" (Buckner et al., 1998; Grill-Spector and Malach, 2001; Kourtzi and Kanwisher, 2001; Winston et al., 2004), whereby the sequential repetition of stimuli sharing a particular feature causes adaptation of neural populations specifically sensitive to that feature, leading to local response decreases. In simple terms, adaptation reflects the degree to which sensory coding mechanisms are common to a given pair of stimuli. For example, in the visual domain, repeated (versus novel) objects elicit reductions in the amount of fMRI activity in extrastriate cortex (Buckner et al., 1998), repetitions of shape (but not contour) induce response decreases in the lateral occipital complex (Kourtzi and Kanwisher, 2001), and repeating identity (but not emotion) across face pairs leads to reduced fMRI activity in fusiform cortex (Winston et al., 2004). Each of these examples demonstrates the role of higher-order visual areas in representing more complex visual information and highlights the utility of cross-adaptation techniques in elucidating mechanisms of sensory coding in the human brain. Importantly, this approach has been effectively used to overcome the inherent spatial limitations of conventional fMRI (Naccache and Dehaene, 2001) and consequently has considerable advantages in the present context, given the likelihood that central odor representations are spatially distributed across primary olfactory cortex (Figure 1).

On each trial, subjects made two successive sniffs to pairs of odorants that varied either in perceptual quality ("lemon-like" or "vegetable-like") or molecular functional group (alcohol or aldehyde), resulting in four odorant-pair conditions: similar quality/same group; similar quality/different group; different quality/same group; and different quality/different group. This paradigm conformed to a 2 × 2 factorial design, enabling us to dissociate perceptual and structural determinants of smell (Figure 2). Critically, the experimental design was fully balanced, controlling for the possibility that the effects could be confounded by variations in intensity, hedonics, or other perceptual dimensions, and ensuring that only quality and structure differed systematically across condition types. We hypothesized that if piriform cortex represents odor quality, independent of functional group, then sequential presentation of qualitatively similar odorant pairs should elicit cross-adapting (decreased) neural activity, by comparison to qualitatively dissimilar pairs. In contrast, structural (group) features of odorants should have no impact on neural cross-adaptation within this region. The paradigm simultaneously enabled an investigation of odorant structure (group) coding in piriform cortex, by testing the impact of functional group repetition on fMRI cross-adaptation in olfactory cortex, irrespective of the underlying odor quality.

Results

Behavioral Data: Analysis of Odor Quality

On the basis of pilot studies, we identified four odorants that shared a prominent "lemon" quality (two alcohols: geraniol and citronellol; two aldehydes: nonanal and undecanal) and four odorants that shared a prominent "vegetable" quality (two alcohols: 1-octen-3-ol and 3-octanol; two aldehydes: trans-2-octenal and

A

		lemon-like
alcohol	{	geraniol (1)
		citronellol (2)
aldehyde	{	nonanal (3)
		undecanal (4)
		vegetable-like
alcohol	{	1-octen-3-ol (5)
		3-octanol (6)
aldehyde	{	tr-2-octenal (7)
		tr,tr-2,4-octadienal (8)

B

Molec. functional group (of 2nd odorant)

Quality (of 2nd odorant)	same	different
similar	1:2 2:1 3:4 4:3 5:6 6:5 7:8 8:7	1:3 3:1 5:7 7:5 1:4 4:1 5:8 8:5 2:3 3:2 6:7 7:6 2:4 4:2 6:8 8:6
different	1:5 5:1 3:7 7:3 1:6 6:1 3:8 8:3 2:5 5:2 4:7 7:4 2:6 6:2 4:8 8:4	1:7 7:1 3:5 5:3 1:8 8:1 3:6 6:3 2:7 7:2 4:5 5:4 2:8 8:2 4:6 6:4

Figure 2. Experimental Design

(A) Stimuli consisted of four odorants each of two quality categories (lemon-like, vegetable-like) and two functional groups (alcohols, aldehydes).

(B) Trial-specific odorant pairings conformed to a 2 × 2 factorial design, with factors "quality" (second odorant similar/different to the first) and "group" (second odorant same/different to the first). Odorant pairs are denoted by numbers 1–8, which refer to stimuli listed in (A). In this fully balanced design, each odorant appeared equal numbers of times as first and second stimulus within each condition.

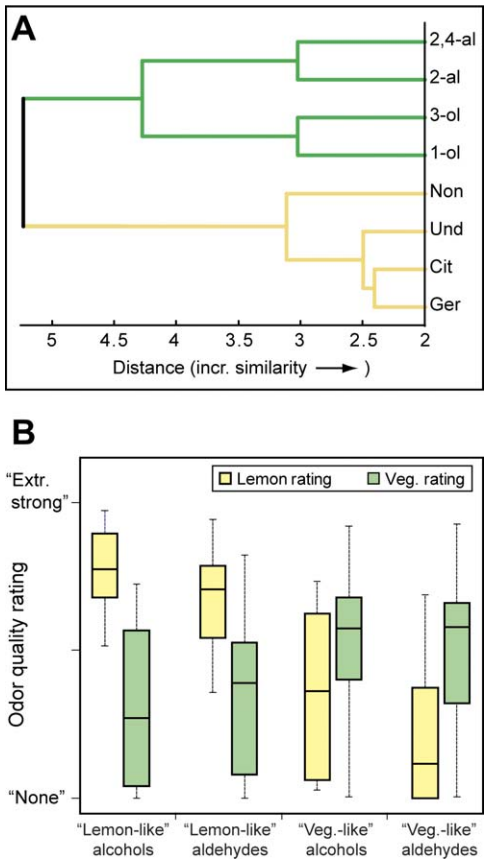

Figure 3. Psychophysical Characterization of Odorants

(A) Hierarchical cluster analysis of odorant similarity. The dendrogram indicates that the odorants cluster into two basic groups, one containing the four "lemon-like" odorants (geraniol [Ger], citronellol [Cit], undecanal [Und], nonanal [Non]; yellow branch of cluster "tree"), the other containing the four "vegetable-like" odorants (1-octen-3-ol [1-ol], 3-octanol [3-ol], 2-octenal [2-al], 2,4-octadienal [2,4-al]; green branch of cluster "tree"), providing an objective basis for categorizing the eight-odorant set into two discrete qualitative categories.

(B) Mean ratings of "lemon" and "vegetable" odor qualities. Boxplots indicate median (central line) and upper and lower quartiles (top and bottom of box, respectively) for each condition. Whiskers denote extent of data between 10th to 90th percentiles. Plots show that subjects rated the "lemon-like" odorants as more akin to lemon (and less akin to vegetable) than the "vegetable-like" odorants, and rated the "vegetable-like" odorants as more akin to vegetable (and less akin to lemon) than the "lemon-like" odorants.

trans,trans-2,4-octadienal). In this way, the eight odorants differed systematically in either perceptual quality (lemon, vegetable) or molecular functional group (alcohols, aldehydes). Note that it is not our intention to imply that the selected stimuli are archetypal representations of lemon (or vegetable) smells, but rather that each set of four odorants contains this lemon (or vegetable) note in common. For example, while geraniol and citronellol are often considered to be "floral" in quality (Arctander, 1994), a majority of our subjects (not to mention Zwaardemaker's [Zwaardemaker, 1895] own classification, depicted in Wise et al., 2000) reported that these compounds were more citrus-like than floral, which may in part be due to contextual effects of presenting it alongside other odorants that smelled more categorically of lemon (Wise et al., 2000). Nevertheless, to document these perceptual distinctions more quantitatively, we collected two sets of psychophysical data from the subjects, described below.

In the first approach, subjects rated the applicability of 146 odor-quality descriptors (Dravnieks, 1985) to each of the eight odorants. Odorant-specific data were then averaged across subjects and entered into a computational analysis of odor quality, using cluster analysis. A graphical representation of this approach is shown in the dendrogram in Figure 3A, where cluster distance (x axis) represents odorant quality similarity. This indicates that the odorants cluster into two basic groups, one containing the four "lemon" odorants, the other containing the four "vegetable" odorants, providing an objective basis for categorizing the eight-odorant set into two discrete qualitative categories.

In the second approach, subjects rated each odorant for its lemon-like quality and its vegetable-like quality along a visual analog scale (Stevenson, 2001). Subjects rated the "lemon-like" odorants as more akin to lemon (and less akin to vegetable) than the "vegetable-like" odorants, and rated the "vegetable-like" odorants as more akin to vegetable (and less akin to lemon) than the "lemon-like" odorants (Figure 3B). There was a significant difference across these rating scores ($\chi^2 = 50.89$; $p < 0.001$; Friedman test). In post hoc comparisons, lemon ratings were significantly higher for "lemon-like" odorants than "vegetable-like" odorants ($Z = -3.52$; $p < 0.001$; Wilcoxon test, two-tailed),

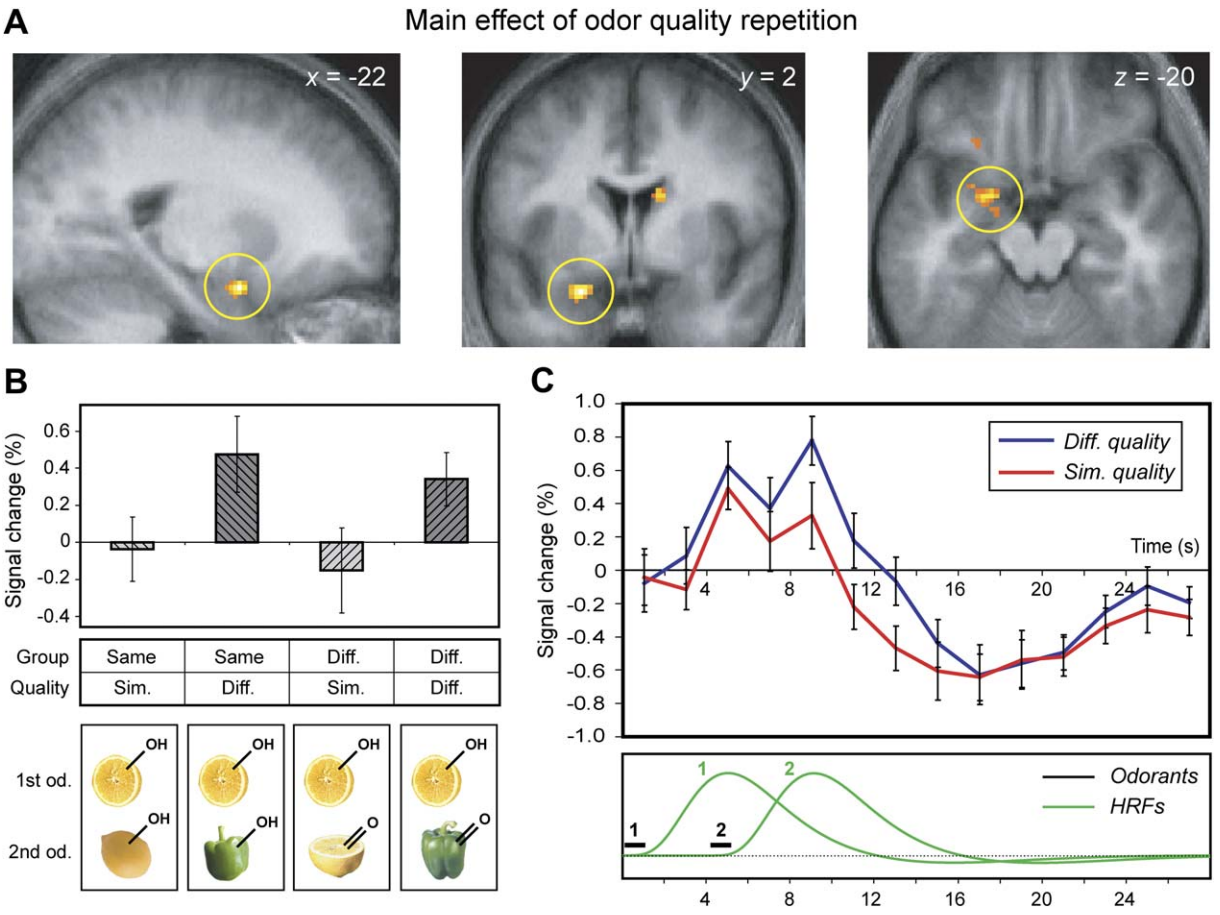

Figure 4. Posterior Piriform Representations of Odor Quality

(A) The main effect of quality repetition revealed significant effects in posterior piriform cortex. The group statistical parametric map (SPM) is displayed on sagittal (left), coronal (middle), and axial (right) sections of the subject-averaged T1-weighted anatomical scan (threshold for display, $p < 0.005$).

(B) Condition-specific plots of the mean activity from the peak posterior piriform voxel. The bottom of the panel shows pictorial examples of the four different conditions (−OH, alcohol; =O, aldehyde).

(C) Group-averaged response time courses for qualitatively similar and different odorant repeats, estimated at 2 s intervals. There is a selective response decrease when the second odorant is similar in quality to the first. Corresponding time courses of odorants and predicted canonical hemodynamic responses (HRFs) (first [1] and second [2] events per trial pair) are shown at the bottom. Depiction of the HRF waveforms is not meant to indicate that these functions were actually used in estimating the time courses in (C); they merely illustrate that the response time courses peak on a timescale predicted by the canonical function, validating the use of canonical HRFs in the primary analysis depicted in (A) and (B).

Error bars indicate mean ± SEM.

whereas vegetable ratings were significantly higher for "vegetable-like" odorants than "lemon-like" odorants ($Z = -2.90$; $p < 0.005$). Moreover, lemon ratings were significantly higher than vegetable ratings for "lemon-like" odorants ($Z = -3.31$; $p < 0.005$), whereas vegetable ratings were significantly higher than lemon ratings for "vegetable-like" odorants ($Z = -2.59$; $p < 0.05$). These findings highlight an effective sculpting of the odor space, permitting us to dissociate quality from structure within the experiment.

Imaging Data: Odor Quality

We next analyzed the neural substrates of fMRI cross-adaptation induced by the odorant set. The first contrast examined the main effect of quality repetition to identify neural representations of odor quality. The comparison of perceptually different to perceptually similar odorant pairs revealed significant cross-adapting (decreased) activity in left posterior piriform cortex ($x = -22$, $y = 2$, $z = -22$; $Z = 4.73$; $p < 0.05$, small-volume corrected [SVC]), spanning the fronto-temporal junction and extending to the anterior margin of amygdala (Figure 4A). Significant response decreases in left hippocampus ($-24, -24, -24$; $Z = 4.34$; $p < 0.05$, SVC) and right orbitofrontal cortex (32, 40, −16; $Z = 3.80$; $p < 0.05$, SVC) were also detected, suggesting that representations of odor quality may be distributed across a wider network of olfactory-related regions, in keeping with prior animal (Tanabe et al., 1975) and human (Royet et al., 1999; Savic et al., 2000; Gottfried and Dolan, 2003) studies of olfactory discrimination and semantic processing. Condition-specific plots of mean activity from the posterior piriform peak indicate that molecular group had little impact on the magnitude of cross-adaptation: qualitatively similar odorant pairs elicited comparable response decreases, irrespective of molecular group (Figure 4B). In

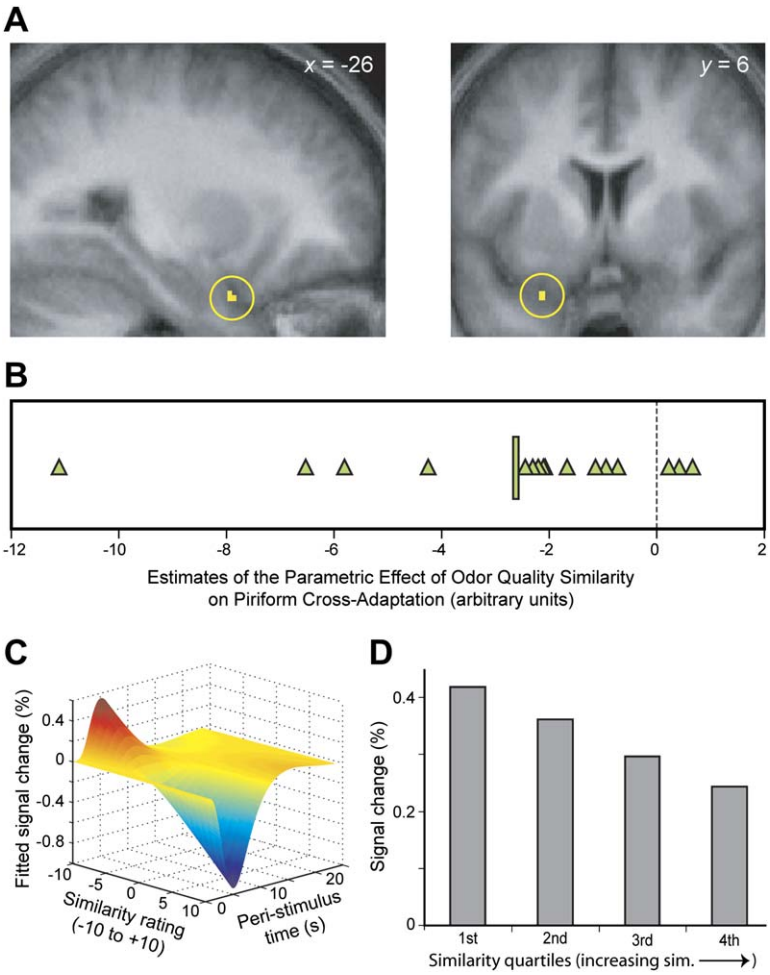

Figure 5. Piriform Cross-Adaptation to Perceived Similarity

(A) In a parametric model of odor quality, posterior piriform activity progressively decreased (increasingly adapted) as ratings of similarity between odorant pairs increased. The group SPM is shown on axial (left) and coronal (right) anatomical sections ($p < 0.005$ for display).

(B) Scatterplots depict single-subject parameter estimates, derived from correlation analyses between similarity ratings of odor quality and neural activity in posterior piriform cortex. These data indicate that most subjects exhibited a negative linear fit, consistent with a progressive decrease in neural activity (cross-adaptation) as odorant pairs are perceived to be more similar in quality. Note the group-averaged parametric effect (short vertical bar) was significantly different from zero (dashed line).

(C) A three-dimensional parametric plot of the group average of each subject's fitted data depicts the influence of perceived similarity on piriform adaptation.

(D) A complementary model that rearranged all second-odorant events into quartiles of increasing perceived similarity, according to each subject's ratings, illustrates posterior piriform sensitivity to this perceptual factor.

keeping with this observation, neither the main effect of structural (group) repetition ($F_{1,15} < 1$; $p = 0.47$) nor the quality-by-group interaction ($F_{1,15} < 1$; $p = 0.97$) were significant. Thus, posterior piriform responses are selectively tuned to qualitative features and are independent of this particular molecular determinant.

For illustration we also estimated the group-averaged response time course in posterior piriform cortex, for qualitatively similar and qualitatively different odorant pairs, collapsed across structure (Figure 4C). Biphasic responses (at 5 and 9 s) corresponded to predicted activation peaks evoked by the first and second odorants in the stimulus pair, with appropriate response lags, suggesting that our technique has sufficient sensitivity to resolve sequentially presented odorants within a 4 s period. Moreover, when the second odorant in the pair was similar in quality to the first, there was a selective decrement in the second response peak, consistent with a physiological specificity to the cross-adaptation effect. A formal analysis of response time course area differences (second versus first odorant) indicated a significant main effect of quality ($F_{1,15} = 4.82$; $p < 0.05$), but no effect of group ($F_{1,15} < 1$; $p = 0.49$) or quality-by-group interaction ($F_{1,15} < 1$; $p = 0.55$). For comparison, posterior piriform time courses to similar and different structure (group) are shown in Figure S1A (see the Supplemental Data available online).

The above results demonstrate a sensitivity of posterior piriform cortex to categorical aspects of odor quality, but do not account for individual variations in odor quality perception, on a trial-by-trial basis. To determine whether perceived similarity between odorant pairs also influenced piriform cross-adaptation, we tested a complementary model in which post hoc similarity ratings for each stimulus pair were entered as parametric regressors. If indeed posterior piriform cortex codes qualitative aspects of odorants, then the prediction is that the cross-adaptation effect would show a sensitivity profile that reflects the degree of perceived similarity. In other words, we would expect a progressive decrease in the effect size (greater cross-adaptation) as a linear function of perceived similarity. Consistent with our prediction, we observed a trend-level effect in a region of posterior piriform cortex (Figure 5A) that overlapped the main effect of quality repetition, albeit at slightly reduced threshold ($-26, 6, -28$; $Z = 2.92$; $p < 0.07$, SVC). Inspection of the single-subject data indicated that 13/16 subjects showed a negative linear fit (Figure 5B), and the group average of each subject's fitted data is depicted parametrically in Figure 5C.

The impact of subjective similarity on piriform cross-adaptation was also illustrated using another fMRI model that partitioned the events into successive quartiles of increasing similarity. This analysis highlighted

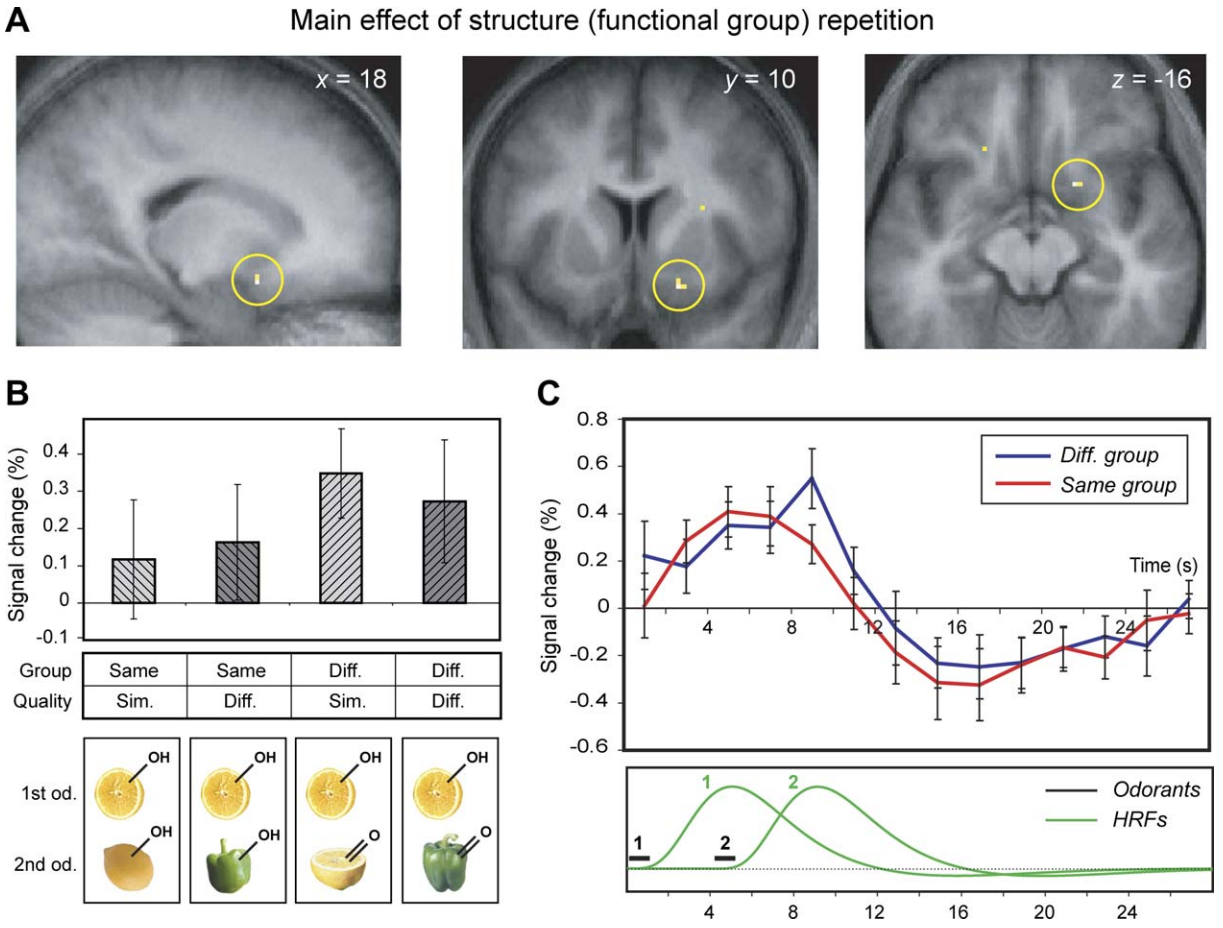

Figure 6. Anterior Piriform Representations of Odorant Structure

(A) The main effect of molecular structure (functional group) repetition yielded significant cross-adaptation in anterior piriform cortex. The group SPM is superimposed on sagittal (left), coronal (middle), and axial (right) T1-weighted sections (display, $p < 0.005$).

(B) Condition-specific plots of the mean activity from the peak anterior piriform voxel indicate that cross-adaptation to repetition of odorant molecular group was largely unaffected by quality.

(C) fMRI response time courses from anterior piriform cortex demonstrate a selective decrease in the signal peak corresponding to the second odorant, upon repetition of structural group.

Error bars indicate mean ± SEM.

the expected enhancement of cross-adaptation (greater response decrement) in piriform cortex with increasing similarity ratings (Figure 5D). Importantly, these plots of mean activity for each quartile were computed using methods completely unconstrained with respect to data fitting (as opposed to Figure 5C) but nevertheless indicate that the relationship between perceived similarity and neural adaptation in posterior piriform cortex is strikingly linear. Overall, the sequence of findings that we describe provides robust evidence that piriform cross-adaptation is sensitive to qualitative features, reinforcing the idea that central representations of perceptual quality are encoded in this region.

Imaging Data: Odorant Structure (Functional Group)

A subsequent contrast examined neural representations of odorant structure, independent of qualitative features, by testing for a main effect of structure (group) repetition. Significant cross-adapting responses in anterior piriform cortex (18, 10, −16; $Z = 3.23$; $p < 0.05$, SVC) were detected in the comparison of structurally similar and structurally different odorant repeats (Figure 6A). Condition-specific plots of mean activity from the anterior piriform peak show that cross-adaptation to odorant functional group was elicited whether or not repetitions were similar in odor quality (Figure 6B). The response in this region was observed in the absence of a significant main effect of quality repetition ($F_{1,15} < 1$; $p = 0.90$) or quality-by-group interaction ($F_{1,15} < 1$; $p = 0.62$). Moreover, the same response profile was still evident (18, 10, −16; $Z = 3.26$; $p < 0.05$, SVC) even when post hoc similarity ratings were included as regressors of no interest, thus making it unlikely that subjective differences in perceptual quality account for the results.

Subject-averaged response time courses from the anterior piriform peak were estimated for similar and different group, each collapsed across quality (Figure 6C). A biphasic response profile was still evident, indicating that the cross-adaptation effect of structurally similar repetitions occurred at a time point corresponding to the predicted response peak of the second (repeated) odorant in the stimulus sequence. In contrast to the

posterior piriform profile, these results demonstrate that neural cross-adaptation in anterior piriform cortex is driven by similarities in one fundamental molecular feature (functional group) and is not reliant on perceptual similarity. In an analysis of response time course area differences, there was a significant main effect of group ($F_{1,15} = 12.13$; $p < 0.05$), but no significant main effect of quality ($F_{1,15} < 1$; $p = 0.56$) or quality-by-group interaction ($F_{1,15} < 1$; $p = 0.92$). The comparative time courses in anterior piriform cortex for similar and different quality are depicted in Figure S1B.

Finally, the Supplemental Material includes additional analyses regarding (1) the potential effect of quality on structure coding in anterior piriform (Figure S2); (2) the influence of molecular determinants (other than functional group) on piriform cross-adaptation; (3) laterality differences between quality and structure coding; and (4) simple comparisons between alcohol/aldehyde groups and between lemon/vegetable qualities. Note that none of these analyses altered the above conclusions in any substantive way.

Imaging Data: Complementary Data Set

The above results provide strong evidence for dissociable neural representations of odor quality and odorant structure (group) in human piriform cortex. To test the robustness of our findings, we extended our hypothesis to another set of eight odorants that systematically varied in molecular functional group and carbon-chain length: four alcohols (C-4, C-6, C-8, C-10) and four aldehydes (C-4, C-6, C-8, C-10) (Figure S3A). Our decision to stratify odorant structure according to molecular functional group and carbon-chain length is motivated by animal data suggesting that both parameters are critical molecular features governing response patterns in olfactory sensory neurons (Zhao et al., 1998; Araneda et al., 2000) and the olfactory bulb (Imamura et al., 1992; Johnson et al., 1998; Rubin and Katz, 1999). A related reason for selecting an orderly, homologous series of odorants was to test the effect of functional group in the absence of other structural/chemical differences, such as branching pattern or bond (saturation) level. Admittedly, such an approach did not provide the same degree of control over odor quality (compared to the primary data set), but it enabled tighter control over molecular properties. We were nevertheless able to examine odor quality coding in this experiment by using perceptual ratings as fMRI regressors of interest (Supplemental Material).

In this complementary study, 18 independent volunteers participated in an olfactory paradigm of fMRI cross-adaptation, similar to the main study. Here, subjects made sequential sniffs and smelled pairs of odorants varying in group and length, as outlined above. The design conformed to a 2 × 3 factorial design (Figure S3B), with factors group (same; different) and carbon-chain length difference (0; 2; 4), enabling us to examine the main effects of group and length. In contrast to the main study, subjects provided online similarity ratings of odor quality following the presentation of each stimulus pair. By assembling the trial-wise similarity ratings into parametric regressors, we were therefore able to explore the neural effect of odor quality within this paradigm.

Behaviorally, subjects perceived odorant pairs to be more dissimilar in quality with differences in functional group, and also with progressive increases in carbon-chain length difference (Figure S4). Predictably, the "same group/0-C length difference" condition (corresponding to identical odorant pairs) showed the greatest amount of similarity, helping to validate the perceptual "sensibility" of the subjects. Statistical analyses indicated a significant difference across conditions ($\chi^2 = 55.32$; $p < 0.001$; Friedman test), and post hoc tests showed significant differences for same and different groups ($Z = -3.46$; $p < 0.001$; Wilcoxon test), 0-C and 2-C length differences ($Z = -3.33$; $p < 0.001$), and 2-C and 4-C length differences ($Z = -3.64$; $p < 0.001$). Notably, these psychophysical results closely align with the behavioral findings of Laska and colleagues (Laska and Teubner, 1999; Laska et al., 2000), confirming that humans are capable of discriminating even minor molecular differences between odorants and that perceptual discrimination improves with increasing differences in carbon-chain length.

In the parametric effect of odor quality, significant cross-adaptation was observed in posterior piriform cortex ($T_{17} = -2.48$; $p < 0.05$). Inspection of the single-subject regression slopes revealed that increases in perceived similarity between odorant pairs were associated with declining piriform activity (greater cross-adaptation) in 15/18 subjects (Figure 7A, triangles). In contrast, in anterior piriform cortex, there was no significant parametric effect of perceived odor quality ($T_{17} = -0.48$; $p = 0.64$) (Figure 7A, diamonds). The selective influence of odor quality on posterior piriform cortex was illustrated using a separate fMRI model, by dividing all odor events (irrespective of group or length) into quartiles of increasing perceptual similarity (Supplemental Material) and then plotting the response time courses. These plots show that in posterior piriform cortex (Figure 7B), progressive increases in odor quality similarity evoke greater cross-adaptation (significant effect of area differences: $F_{2.73,43.65} = 7.96$; $p < 0.001$), whereas in anterior piriform cortex (Figure 7C), no systematic relationship between quality similarity and the level of cross-adaptation was apparent ($F_{2.23,37.94} < 1$; $p = 0.56$).

Alternatively, the effect of functional group repetition revealed significant cross-adaptation in anterior piriform cortex ($F_{1,17} = 6.59$; $p < 0.05$), in the absence of an effect of carbon-chain length difference ($F_{1.77,30.05} < 1$; $p = 0.95$) or a group-by-length interaction ($F_{1.49,25.28} < 1$; $p = 0.96$). The response time courses in anterior piriform cortex highlight the selective decline in odorant-evoked activity when the same (versus different) functional group was presented (Figure 8A). Analysis of area differences (second versus first odorant) showed a significant effect of group ($F_{1,17} = 21.87$; $p < 0.001$), but not for length or the interaction (all p values > 0.05). These results contrast with the response profile in posterior piriform cortex, in which there was no significant effect of group ($F_{1,17} < 1$; $p = 0.56$), length ($F_{1.64,\ 27.96} < 1$; $p = 0.73$), or interaction ($F_{1.9,32.36} < 1$; $p = 0.48$), and the corresponding time course plots (Figure 8B) do not suggest any systematic effect of group or length on posterior piriform cross-adaptation (no significant area differences for group, length, or the interaction; all p values > 0.05).

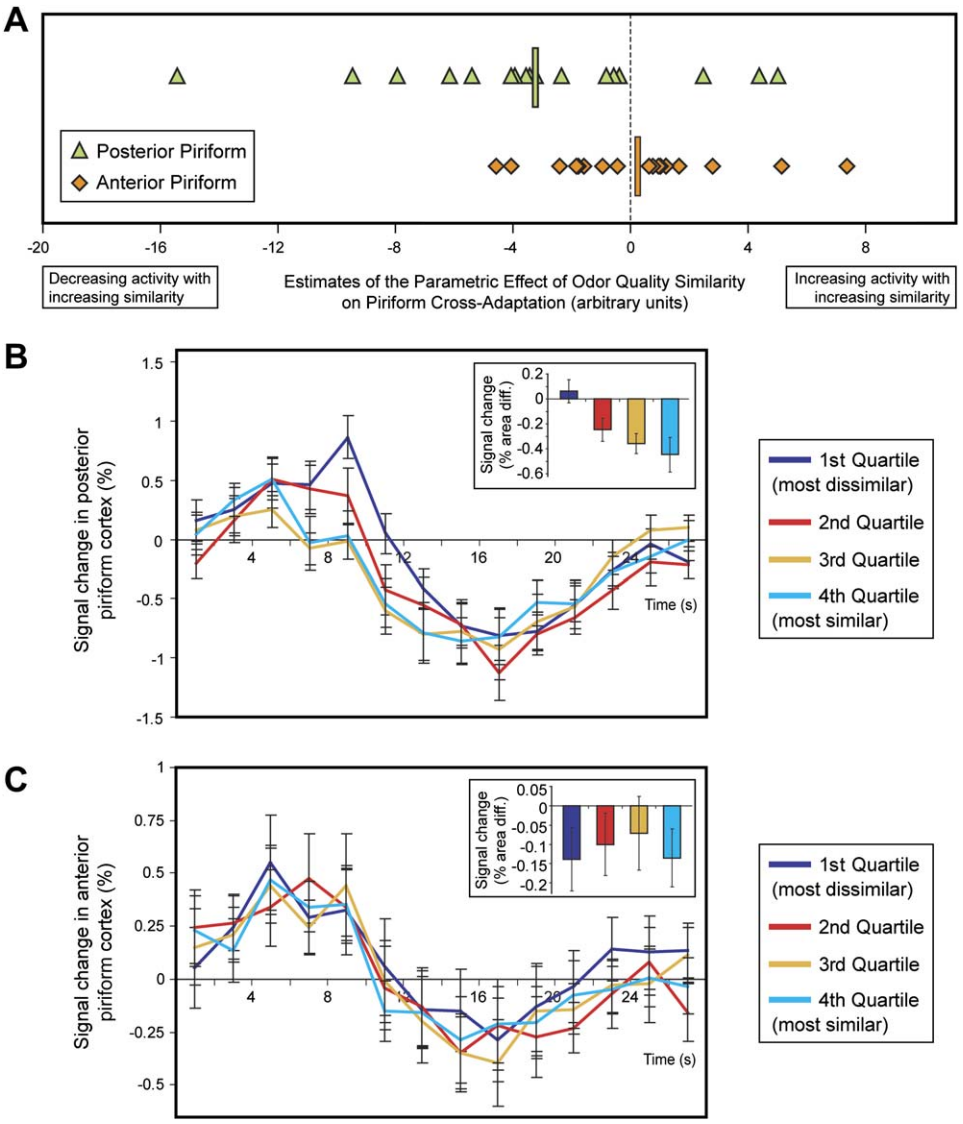

Figure 7. Complementary Study: Odor Quality Coding in Posterior Piriform Cortex

(A) In the parametric effect of odor quality, scatterplots of the single-subject regression slopes indicate that most subjects exhibited a negative linear fit between quality similarity ratings and neural activity in posterior piriform cortex, and the group-averaged mean effect (short vertical bar) significantly differed from zero (dashed line). By comparison, such a pattern was not consistently observed in anterior piriform cortex, and the mean effect was not significantly different from zero. Note the exclusion of one subject outlier (<3 SD below the mean) from the plots had no substantive effect on the statistical analyses.

(B and C) Time course plots show that increasing quality similarity (across successive quartiles) elicited greater cross-adaptation in posterior piriform cortex (B), but no such relationship was manifest in anterior piriform cortex (C). Area differences for each similarity quartile, computed from the time course plots, illustrate progressive adaptation in posterior (but not anterior) piriform cortex as a function of quality ([B and C], insets).

Error bars indicate mean ± SEM.

Note that while subjects perceived "different group" and "same group" conditions as qualitatively different, we consider it unlikely that such differences actually underscored the effect of functional group in anterior piriform (see Supplemental Material). The absence of a length effect in piriform cortex is also discussed in the Supplemental Material.

In summary, these additional findings are in close agreement with the primary data set, confirming the double dissociation of odor quality and odorant structure (functional group) in posterior and anterior piriform cortex, respectively.

Discussion

Olfactory cross-adaptation has been previously used to characterize structure-quality relationships from a psychophysical perspective (Moncrieff, 1956; Engen and Lindstrom, 1963; Cain, 1970; Todrank et al., 1991; O'Connell et al., 1994; Pierce et al., 1996). The central tenet is that cross-adaptation reflects the degree to which coding mechanisms are shared by a given pair of odorants. The evidence presented here indicates that fMRI cross-adaptation can be successfully used to delineate odor coding mechanisms in human olfactory cortex.

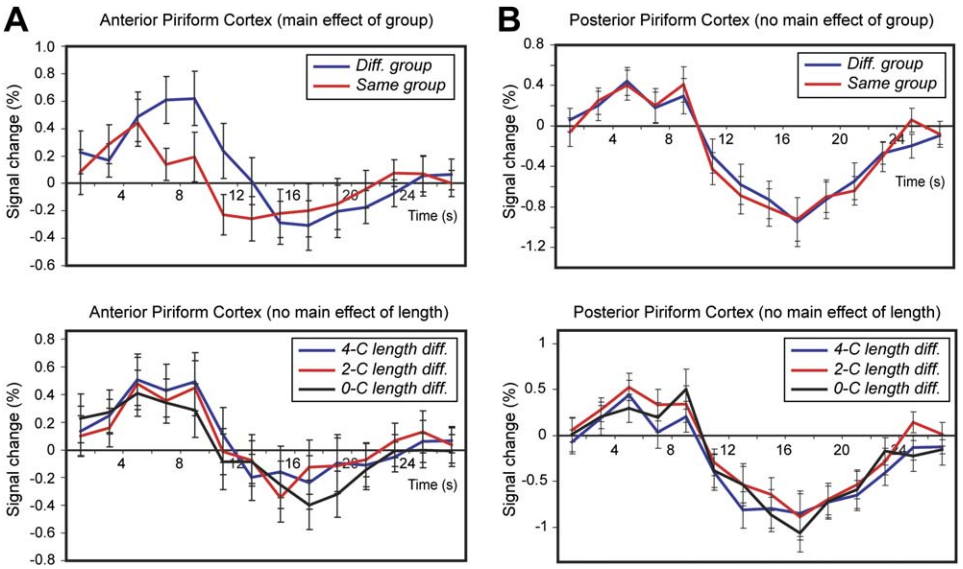

Figure 8. Complementary Study: Odorant Structure (Group) Coding in Anterior Piriform Cortex

(A) Response time courses in anterior piriform cortex reveal a significant effect of functional group (collapsed across carbon-chain length), but not of length (collapsed across group).

(B) By comparison, in posterior piriform cortex, neither functional group nor length evoked significant cross-adaptation.

Error bars indicate mean ± SEM.

By implementing a balanced factorial design (cf. Figure 2), we were able to disentangle the elements of odor quality and odorant structure (functional group) within a single experiment. Our data highlight a double dissociation of odor coding in posterior (quality) and anterior (functional group) subregions of piriform cortex. Importantly, the fact that each odorant appeared equal numbers of times as first and second stimulus within each condition type helped control for the possibility that the findings could be confounded by item-specific differences in intensity, hedonics, or other perceptual features. Moreover, the demonstration of these effects across two separate experiments reinforces the idea that human piriform cortex encodes dissociable neural representations of odor quality and odorant structure and validates the generalizability of our results.

It is worth noting that peripheral mechanisms could possibly contribute to the piriform cross-adaptation effects described here. That is, to the extent that the second odorant smells similar to the first, it could theoretically be more difficult to detect due to peripheral sensory adaptation, which could lead to an observed response decrease in piriform cortex, irrespective of central adaptation processes. Such a mechanism cannot be entirely ruled out (and would in fact be of considerable interest if qualitatively similar odors differing in chemical class induced cross-adaptation at the sensory receptor level). However, we consider this unlikely, because behavioral measures of detection accuracy and reaction time did not differ for the main effect of quality repetition or structure (group) repetition, nor were respiratory measures of sniff volume significantly different (all p values > 0.05, repeated-measures ANOVA). We would argue that if peripheral adaptation were playing an important role, subjects would be less accurate and slower to detect odorant pairs similar in quality and that they would take deeper sniffs for similar-quality odorants, but these effects were not observed. Therefore, we think the likelihood is low that peripheral habituation underscored the piriform response profiles.

The presence of dual olfactory representations (structure and quality) within discrete piriform areas accords with its known anatomical organization. An afferent projection from olfactory bulb predominantly terminates in anterior piriform cortex, whereas major inputs to posterior piriform cortex originate from associational fiber systems arising elsewhere (Haberly, 1998; Wilson and Sullivan, 2003). In keeping with functional organizational principles of visual and auditory cortices, it seems likely that anterior piriform cortex, as the initial relay from olfactory bulb, is a recipient of structure-based information. Indeed, animal studies support the likelihood that anterior piriform cortex provides a biological substrate for odorant structure codes. Individual receptor neurons have been shown to target distinct patches within anterior piriform cortex (Zou et al., 2001), and bulbar afferents to this same piriform region exhibit a modest degree of spatial organization that is apparently independent of odor quality (Ojima et al., 1984; Cattarelli et al., 1988; Illig and Haberly, 2003). More recent work shows an overlap of c-Fos expression patterns in rodent anterior piriform cortex for structurally related odorants (Zou et al., 2005). Such data highlight a plausible mechanism by which lower-level areas would convey structure-based information to anterior piriform cortex. These anterior (structure) codes would then be integrated posteriorly into more highly processed representations of odor quality. The concept of functional heterogeneity along an anterior-posterior axis, as evident in our findings, agrees with electrophysiological and optical imaging data in animals, which indicate preferential response plasticity in posterior (versus anterior) piriform cortex

(Wilson and Sullivan, 2003). Such a mechanism would be especially important to the encoding of quality-based odor representations that depend to a considerable extent upon learning and experience for their formation.

What might be the advantage of retaining cortical representations of structure, in the absence of qualitative information? We speculate that the preservation of such codes would help ensure stimulus fidelity of the original sensory input. This would be particularly important in cases where perceived quality is not always a reliable marker of an odor event, for example, with changes in odor concentration, background odor composition, or exposure duration. The encoding of odorant structure may also reflect the unique organization of the olfactory system, which, unlike all other modalities, lacks a requisite thalamic relay between sensory receptor and cortex. It is therefore possible that anterior piriform cortex might subserve a role otherwise provided by the thalamus, including detection, analysis, and transformation of a sensory signal (Sherman and Guillery, 1996). The successful execution of these functions would be contingent upon access to lower-level information arriving from olfactory receptor neurons and bulb. A final consideration is that odorant molecular group might help direct feeding-related behaviors. As one supporting example, it has been shown that fruit maturation induces pronounced changes in the relative proportions of functional-group categories, with progressive increases in acids and esters and decreases in aldehydes (Menager et al., 2004). In this manner, cortical access to structure information would provide a ready means of detecting differences in the overall balance of odorant molecular groups, which could help guide the selection (or avoidance) of nutritionally favorable foodstuffs.

Increasing evidence highlights the influence of molecular features on odor discrimination and neural coding in olfactory bulb (e.g., Linster et al., 2001). The present demonstration of quality-based representations in posterior piriform cortex, independent of odorant functional group, suggests the current emphasis on molecular parameters may overlook alternative potential coding mechanisms. How odor quality maps might become established in piriform cortex remains unclear, though one possibility is that complex configurations of structural features are translated by olfactory receptors into integrated odor percepts (Malnic et al., 1999). However, the fact that our findings spanned numerous odorants differing in group, length, saturation, and branching pattern defies a straightforward correspondence between molecular and perceptual odor dimensions. It is also possible that biologically relevant odors (e.g., fruit or vegetable smells), irrespective of their underlying molecular composition, are encoded at the level of posterior piriform cortex as odor-object categories, akin to visual object forms in human ventral temporal cortex. Finally, piriform representations of odor quality could be established through semantic associations, sensory context, and perceptual learning (Wilson, 2003; Wilson and Sullivan, 2003), perhaps via re-entrant influences from such centers as OFC and hippocampus (Gottfried and Dolan, 2003). Regardless of the actual mechanism, our findings raise the interesting possibility that quality-based information in piriform cortex might refine the receptive-field organization within olfactory bulb via centrifugal feedback, thereby imposing an epigenetic constraint on "bottom-up" attempts to define bulbar maps on the basis of structural properties alone. We suggest that in the absence of characterizing the coding principles underpinning perceived odor quality, efforts to understand how the brain transforms one airborne compound into the smell of chocolate, and another into cheese, will remain unresolved.

Experimental Procedures

Odorants and Odorant Delivery

We selected eight odorants (Sigma-Aldrich) that systematically varied in molecular structure and perceptual quality. There were four lemon-like odorants comprising two alcohols (geraniol; citronellol) and two aldehydes (nonanal; undecanal), and four vegetable-like odorants comprising two alcohols (1-octen-3-ol; 3-octanol) and two aldehydes (trans-2-octenal; trans,trans-2,4-octadienal). Odorants (absorbed onto diethylphthalate pellets) were presented using an MRI-compatible computer-controlled olfactometer (airflow, 2 L/min), as previously described (Gottfried et al., 2002).

Paradigm

Sixteen healthy right-handed volunteers (mean age, 25 years; eight women) provided informed consent to take part in the study, which was approved by the Joint Ethics Committee of the Institute of Neurology and the National Hospital for Neurology and Neurosurgery. Subjects participated in an olfactory version of fMRI cross-adaptation, in which pairs of odorants were successively presented on each trial. There were four critical odorant-pair conditions, enabling independent manipulation of odor quality and odorant structure (group): similar quality/same group; similar quality/different group; different quality/same group; and different quality/different group. This conformed to a 2 × 2 factorial design, with factors quality (similar/different) and group (same/different). In addition, an "identical" condition (second odorant same as the first) provided a maximal envelope of cross-adaptation, and a "blank" condition, whereby the second odorant in the pair was not delivered, was included for subjects to perform an odor detection task (see below).

On each trial, subjects made a first sniff after viewing the words "SNIFF NOW" back-projected onto a headbox mirror. The sniff instruction terminated after 1 s, signaling subjects to cease sniffing and exhale. After a 3.2 s delay, the sniff cue reappeared, prompting a second sniff (resulting in a 4.2 s sniff-cue interval). Following this, subjects pressed one of two buttons to indicate whether the second odorant was present or absent. Trials recurred with a mean stimulus-onset asynchrony of 24.3 s (± variable jitter between 0.54–4.32 s). The experiment was divided into two 25 min fMRI sessions. Per session there were eight trials each of the six conditions. Over the experiment, all eight odorants were equally distributed as first and second stimulus across all conditions (except for the "blank" condition). Odorant delivery sequence was pseudorandomized, with the constraint that no odorant was presented more than twice in successive trials. Stimulus presentation was controlled using Cogent2000 (Wellcome Dept., London, UK), as implemented in Matlab (Mathworks, Natick, MA).

Behavior

Reaction times and accuracy of odor detection (second sniff) were recorded online and averaged across condition types. Respirations were also monitored during scanning, and measurements of sniff volume (second sniff) were averaged across conditions (Gottfried et al., 2002). At the end of scanning, subjects rated the applicability of 146 odor-quality descriptors (Dravnieks, 1985) to each odorant. Odorant-specific data were then averaged across subjects and entered into hierarchical cluster analysis. Clusters were grouped according to similarity using an "average linkage" algorithm (average distances between all pairs of objects in two clusters), following standard procedures in Matlab. Post hoc ratings of odor similarity were also collected for all pairwise stimulus combinations using a visual analog scale with anchors "extremely different" and "identical."

Post hoc ratings of perceived odor quality (separately for lemon and vegetable qualities) were collected for each odorant, with anchors "none" and "extremely strong" (Stevenson, 2001). Subjects viewed these scales at the same time that the words "lemon rating" or "vegetable rating" appeared on the computer screen. In the case of lemon ratings, for example, "none" referred to the complete absence of lemon quality, whereas "extremely strong" referred to an extremely strong presence of lemon quality. Finally, ratings of odor intensity and odor valence were collected, with anchors "none" and "extremely strong" (intensity), or "extremely like" and "extremely dislike" (valence).

Imaging

Gradient-echo T2*-weighted echoplanar images (EPI) were acquired with blood oxygen level-dependent (BOLD) contrast on a Siemens Sonata 1.5 T MRI scanner (555 volumes/session, 24 slices/volume), using a tilted sequence protocol to improve signal resolution in medial temporal and orbitofrontal lobes (Deichmann et al., 2003). This sequence provided adequate coverage of critical olfactory areas including piriform and orbitofrontal cortices. Imaging parameters were: TR, 2.16 s; TE, 35 ms; slice thickness, 2 mm; gap, 1 mm; in-plane resolution, 3 × 3 mm; field-of-view, 192 mm. High-resolution (1 × 1 × 1 mm) T1-weighted anatomical scans were acquired after functional scanning. These were coregistered to the functional EPI, normalized, and averaged across subjects to aid localization.

fMRI Data Preprocessing

The fMRI data were preprocessed using SPM2 (Wellcome Dept., London, UK). After the first eight "dummy" volumes were discarded to permit T1 relaxation, images were spatially realigned to the first volume of the first session, followed by spatial normalization to a standard EPI template, resulting in a functional voxel size of 2 × 2 × 2 mm. Normalized images were smoothed using a 6 mm (FWHM) kernel, which renders the response at each brain voxel a local regional average. This has the advantage of permitting group comparison and renders the data amenable to statistical inference using Gaussian random-field theory. Thus, in referring to a "peak" voxel, we refer to the maximum of a significant regional response—not the response for the voxel itself.

fMRI Data Analysis

Following image preprocessing, the event-related fMRI data were analyzed in SPM2 using the general linear model (GLM) in combination with established procedures (Friston et al., 1995). In the first step, seven vectors of onset times corresponding to each of the condition types were created: (1) all first odorant events; (2) second odorant events, sim. quality/same group to the first odorant; (3) second odorant, diff. quality/same group; (4) second odorant, sim. quality/diff. group; (5) second odorant, diff. quality/diff. group; (6) second odorant, identical to the first odorant; and (7) no second odorant ("blank"). The seven onset vectors were then encoded as stick (δ) functions to assemble seven event-related regressors of interest for inclusion in the GLM. The regressors were convolved with a synthetic hemodynamic response function (HRF), and the inclusion of temporal and dispersion derivatives allowed for variations in HRF latency and width. Regressors of no interest included six movement-related regressors (derived from realignment) and a high-pass filter (1/128 Hz) to remove low-frequency drifts. Temporal autocorrelation was modeled using an AR(1) process.

Model estimation proceeded in two stages. In the first stage, condition-specific experimental effects (parameter estimates, or regression coefficients, pertaining to the height of the canonical HRF) were obtained via the GLM in a voxel-wise manner for each subject. In the second (random-effects) stage, subject-specific linear contrasts of these parameter estimates were entered into a series of one-sample t tests, each constituting a group-level statistical parametric map. To assess the relative response amplitude of the BOLD signal for each condition type, parameter estimates were converted to percent signal change by scaling relative to the whole-brain mean signal computed over the entire session.

There were four principal contrasts. (1) The general effect of odor stimulation was tested using a (+1) contrast for the regressor modeling "all first odorant events." This was orthogonal to the other six "second odorant" regressors and was used as an inclusive mask (at $p < 0.05$, uncorrected) to delimit the activations in contrasts (2), (3), and (4) described below. (2) The main effect of quality repetition: [second odorant diff. quality/same group + second odorant diff. quality/diff. group] − [second odorant sim. quality/same group + second odorant sim. quality/diff. group]. This tested for regional responses that decreased when the second odorant was qualitatively similar to the first odorant, irrespective of group. (3) The main effect of functional group repetition: [second odorant sim. quality/diff. group + second odorant diff. quality/diff. group] − [second odorant sim. quality/same group + second odorant diff. quality/same group]. This tested for regional responses that decreased when the second odorant shared the same group as the first odorant, irrespective of quality. (4) The interaction of quality and group: [second odorant diff. quality/same group − second odorant sim. quality/same group] − [second odorant diff. quality/diff. group − second odorant sim. quality/diff. group]. This tested for regional responses that preferentially decreased when the second odorant was both structurally and qualitatively similar to the first odorant.

Activations are reported in a limited set of brain areas where we had a priori hypotheses, including anterior and posterior piriform cortex, orbitofrontal cortex, and hippocampus. These were corrected for multiple comparisons across small volumes of interest (Worsley et al., 1996) ("small volume correction" [SVC]), using anatomical masks assembled in MRIcro (http://www.mricro.com), with reference to a human brain atlas (Mai et al., 1997). Significance was set at a threshold of $p < 0.05$, corrected. Reported voxels conform to MNI (Montreal Neurological Institute) coordinate space.

The critical contrasts are depicted as group-level statistical parametric maps (Figures 4A and 6A) and as plots of mean percent signal change from the peak voxels (centroids of maximal activation) for each relevant condition (Figures 4B and 6B). Because the "identical" condition represented the maximal extent of adaptation, it was used as a reference condition, and the condition-specific plots of activity in Figures 4B and 6B are shown relative to this.

Response Time Courses

A finite-impulse-response (FIR) model was estimated in SPM2 to illustrate condition-specific response time courses from the piriform maxima identified in the primary SPM model. In this way it complemented the data in Figures 4B and 6B showing condition-specific mean activity levels from these same brain regions. The FIR analysis was completely unconstrained (unfitted) and made no assumptions about the shape of the temporal response. The time courses for each of the condition types were characterized using a set of impulse response functions (14 bins of 2 s duration; length in time, 28 s) with the first bin aligned to the initial onset of each event.

Condition-specific impulse responses from each of the 14 basis functions were estimated in a voxel-wise manner per subject. Depicted time courses are the group-averaged set of stimulus-led responses for each critical comparison from the "quality" peak in posterior piriform (Figure 4C, different and similar quality) and the "structure" peak in anterior piriform (Figure 6C, different and same group). For comparison, the time courses from posterior piriform (Figure S1A, different and same group) and anterior piriform (Figure S1B, different and similar quality) are also depicted. Note that while certain conditions appear to have slightly different starting points, there were no significant differences between conditions at this first time point (for plots in Figures 4, 6, 7, and 8 and in Figure S1: all p values > 0.05).

Time course plots were also submitted to statistical analysis, by calculating subject-specific "areas under the curve" for the "quality" peak in posterior piriform and the "structure" peak in anterior piriform. Because the critical factor was the response change from first to second sniff (reflecting within-condition cross-adaptation), areas were separately computed for the first sniff (area between 3–7 s) and the second sniff (area between 7–11 s), and then area differences were obtained for each of the critical conditions. The data were entered into a quality-by-group ANOVA for statistical testing.

Parametric fMRI Model of Perceived Odorant Similarity

The parametric model was tested by compiling all "same group" events into one regressor, and all "different group" events into another regressor, irrespective of the "quality" factor. These were then multiplied by each subject's post hoc ratings of odorant-pair

similarity, on a trial-by-trial basis, to modulate the amplitude of each event regressor (effectively, a condition by rating interaction). fMRI model estimation was otherwise identical to the primary analysis, and the parametric effect was examined at the random-effects level by testing the (+1) contrast for the parametric regressors. Although there is no a priori reason to suspect that ratings of odor similarity and levels of piriform adaptation should be linearly correlated, we reasoned that a linear relationship would be the most parsimonious way to model the data (and indeed is effective in capturing a wide range of physiological responses). The basic hypothesis was that odorant pairs judged to be most similar in quality would elicit the greatest amount of cross-adaptation, whereas odorant pairs judged to be least similar in quality would elicit the least amount of cross-adaptation. Therefore, we anticipated that these effects would be reasonably captured by a linear term, even if the underlying psychophysiological relationship was not entirely linear.

Additional fMRI Model of Perceived Odorant Similarity

An additional model was tested by rearranging the second-odorant events into successive quartiles of increasing similarity, according to each subject's own ratings. This resulted in 16 events per quartile. As in the primary analysis, δ functions (corresponding to the event onset times for each quartile) were convolved with a canonical HRF to form condition-specific regressors of interest, and parameter estimates for each condition were obtained in SPM2. Percent signal change from the peak voxel identified in the parametric model (above) was then computed for each quartile.

Complementary Experiment of Functional Group versus Carbon Chain Length

See Supplemental Experimental Procedures.

Supplemental Data

The Supplemental Data for this article can be found online at http://www.neuron.org/cgi/content/full/49/3/467/DC1/.

Acknowledgments

We thank N. Ravel for odor pellets and J. Kilner for helpful advice. This research was supported by a Physician-Scientist Postdoctoral Fellowship Grant from the Howard Hughes Medical Institute (J.A.G.) and a Wellcome Trust Programme Grant (R.J.D.).

Received: August 24, 2005
Revised: October 19, 2005
Accepted: January 10, 2006
Published: February 1, 2006

References

Amoore, J.E. (1972). Molecular Basis of Odor (Springfield, IL: Charles C. Thomas).

Araneda, R.C., Kini, A.D., and Firestein, S. (2000). The molecular receptive range of an odorant receptor. Nat. Neurosci. *3*, 1248–1255.

Arctander, S. (1994). Perfume and Flavor Chemicals (Aroma Chemicals) (Carol Stream, IL: Allured Publishing Company).

Baylis, G.C., and Rolls, E.T. (1987). Responses of neurons in the inferior temporal cortex in short term and serial recognition memory tasks. Exp. Brain Res. *65*, 614–622.

Buck, L., and Axel, R. (1991). A novel multigene family may encode odorant receptors: a molecular basis for odor recognition. Cell *65*, 175–187.

Buckner, R.L., Goodman, J., Burock, M., Rotte, M., Koutstaal, W., Schacter, D., Rosen, B., and Dale, A.M. (1998). Functional-anatomic correlates of object priming in humans revealed by rapid presentation event-related fMRI. Neuron *20*, 285–296.

Cain, W.S. (1970). Odor intensity after self-adaptation and cross-adaptation. Percept. Psychophys. *7*, 271–275.

Cain, W.S., and Polak, E.H. (1992). Olfactory adaptation as an aspect of odor similarity. Chem. Senses *17*, 481–491.

Cattarelli, M., Astic, L., and Kauer, J.S. (1988). Metabolic mapping of 2-deoxyglucose uptake in the rat piriform cortex using computerized image processing. Brain Res. *442*, 180–184.

Counet, C., Callemien, D., Ouwerx, C., and Collin, S. (2002). Use of gas chromatography-olfactometry to identify key odorant compounds in dark chocolate. Comparison of samples before and after conching. J. Agric. Food Chem. *50*, 2385–2391.

Deichmann, R., Gottfried, J.A., Hutton, C., and Turner, R. (2003). Optimized EPI for fMRI studies of the orbitofrontal cortex. Neuroimage *19*, 430–441.

Dravnieks, A. (1985). Atlas of Odor Character Profiles (Philadelphia: ASTM).

Engen, T., and Lindstrom, C.O. (1963). Cross-adaptation to the aliphatic alcohols. Am. J. Psychol. *76*, 96–102.

Friston, K.J., Holmes, A.P., Worsley, K.J., Poline, J.-P., Frith, C.D., and Frackowiak, R.S.J. (1995). Statistical parametric maps in functional imaging: a general linear approach. Hum. Brain Mapp. *2*, 189–210.

Gottfried, J.A., and Dolan, R.J. (2003). The nose smells what the eye sees: crossmodal visual facilitation of human olfactory perception. Neuron *39*, 375–386.

Gottfried, J.A., Deichmann, R., Winston, J.S., and Dolan, R.J. (2002). Functional heterogeneity in human olfactory cortex: an event-related functional magnetic resonance imaging study. J. Neurosci. *22*, 10819–10828.

Grill-Spector, K., and Malach, R. (2001). fMR-adaptation: a tool for studying the functional properties of human cortical neurons. Acta Psychol. (Amst.) *107*, 293–321.

Haberly, L.B. (1998). Olfactory cortex. In The Synaptic Organization of the Brain, G.M. Shepherd, ed. (New York: Oxford University Press), pp. 377–416.

Haberly, L.B., and Bower, J.M. (1989). Olfactory cortex: model circuit for study of associative memory? Trends Neurosci. *12*, 258–264.

Henning, H. (1916). Der Geruch (Leipzig, Germany: Barth).

Illig, K.R., and Haberly, L.B. (2003). Odor-evoked activity is spatially distributed in piriform cortex. J. Comp. Neurol. *457*, 361–373.

Imamura, K., Mataga, N., and Mori, K. (1992). Coding of odor molecules by mitral/tufted cells in rabbit olfactory bulb. I. Aliphatic compounds. J. Neurophysiol. *68*, 1986–2002.

Johnson, B.A., Woo, C.C., and Leon, M. (1998). Spatial coding of odorant features in the glomerular layer of the rat olfactory bulb. J. Comp. Neurol. *393*, 457–471.

Kay, L.M., and Freeman, W.J. (1998). Bidirectional processing in the olfactory-limbic axis during olfactory behavior. Behav. Neurosci. *112*, 541–553.

Kourtzi, Z., and Kanwisher, N. (2001). Representation of perceived object shape by the human lateral occipital complex. Science *293*, 1506–1509.

Laska, M., and Teubner, P. (1999). Olfactory discrimination ability for homologous series of aliphatic alcohols and aldehydes. Chem. Senses *24*, 263–270.

Laska, M., Ayabe-Kanamura, S., Hubener, F., and Saito, S. (2000). Olfactory discrimination ability for aliphatic odorants as a function of oxygen moiety. Chem. Senses *25*, 189–197.

Linster, C., Johnson, B.A., Yue, E., Morse, A., Xu, Z., Hingco, E.E., Choi, Y., Choi, M., Messiha, A., and Leon, M. (2001). Perceptual correlates of neural representations evoked by odorant enantiomers. J. Neurosci. *21*, 9837–9843.

Macdonald, A. (1922). An experimental study of Henning's system of olfactory qualities. Am. J. Psychol. *33*, 535–553.

Mai, J.K., Assheuer, J., and Paxinos, G. (1997). Atlas of the Human Brain (San Diego: Academic Press).

Malnic, B., Hirono, J., Sato, T., and Buck, L.B. (1999). Combinatorial receptor codes for odors. Cell *96*, 713–723.

Menager, I., Jost, M., and Aubert, C. (2004). Changes in physicochemical characteristics and volatile constituents of strawberry (Cv. Cigaline) during maturation. J. Agric. Food Chem. *52*, 1248–1254.

Miller, E.K., Li, L., and Desimone, R. (1991). A neural mechanism for working and recognition memory in inferior temporal cortex. Science *254*, 1377–1379.

Moncrieff, R.W. (1956). Olfactory adaptation and odor likeness. J. Physiol. *133*, 301–316.

Moncrieff, R.W. (1967). The Chemical Senses (London: Leonard Hill).

Mouly, A.M., Fort, A., Ben-Boutayab, N., and Gervais, R. (2001). Olfactory learning induces differential long-lasting changes in rat central olfactory pathways. Neuroscience *102*, 11–21.

Naccache, L., and Dehaene, S. (2001). The priming method: imaging unconscious repetition priming reveals an abstract representation of number in the parietal lobes. Cereb. Cortex *11*, 966–974.

O'Connell, R.J., Stevens, D.A., and Zogby, L.M. (1994). Individual differences in the perceived intensity and quality of specific odors following self- and cross-adaptation. Chem. Senses *19*, 197–208.

Ojima, H., Mori, K., and Kishi, K. (1984). The trajectory of mitral cell axons in the rabbit olfactory cortex revealed by intracellular HRP injection. J. Comp. Neurol. *230*, 77–87.

Pierce, J.D., Jr., Wysocki, C.J., Aronov, E.V., Webb, J.B., and Boden, R.M. (1996). The role of perceptual and structural similarity in cross-adaptation. Chem. Senses *21*, 223–237.

Polak, E.H. (1973). Multiple profile-multiple receptor site model for vertebrate olfaction. J. Theor. Biol. *245*, 175–184.

Royet, J.P., Koenig, O., Gregoire, M.C., Cinotti, L., Lavenne, F., Le Bars, D., Costes, N., Vigouroux, M., Farget, V., Sicard, G., et al. (1999). Functional anatomy of perceptual and semantic processing for odors. J. Cogn. Neurosci. *11*, 94–109.

Rubin, B.D., and Katz, L.C. (1999). Optical imaging of odorant representations in the mammalian olfactory bulb. Neuron *23*, 499–511.

Savic, I., Gulyas, B., Larsson, M., and Roland, P. (2000). Olfactory functions are mediated by parallel and hierarchical processing. Neuron *26*, 735–745.

Schoenbaum, G., and Eichenbaum, H. (1995). Information coding in the rodent prefrontal cortex. I. Single-neuron activity in orbitofrontal cortex compared with that in pyriform cortex. J. Neurophysiol. *74*, 733–750.

Sherman, S.M., and Guillery, R.W. (1996). Functional organization of thalamocortical relays. J. Neurophysiol. *76*, 1367–1395.

Stevenson, R.J. (2001). Associative learning and odor quality perception: how sniffing an odor mixture can alter the smell of its parts. Learn. Motiv. *32*, 154–177.

Tanabe, T., Iino, M., and Takagi, S.F. (1975). Discrimination of odors in olfactory bulb, pyriform-amygdaloid areas, and orbitofrontal cortex of the monkey. J. Neurophysiol. *38*, 1284–1296.

Todrank, J., Wysocki, C.J., and Beauchamp, G.K. (1991). The effects of adaptation on the perception of similar and dissimilar odors. Chem. Senses *16*, 467–482.

Touhara, K., Sengoku, S., Inaki, K., Tsuboi, A., Hirono, J., Sato, T., Sakano, H., and Haga, T. (2000). Functional identification and reconstitution of an odorant receptor in single olfactory neurons. Proc. Natl. Acad. Sci. USA *96*, 4040–4045.

Wilson, D.A. (2003). Rapid, experience-induced enhancement in odorant discrimination by anterior piriform cortex neurons. J. Neurophysiol. *90*, 65–72.

Wilson, D.A., and Stevenson, R.J. (2003). The fundamental role of memory in olfactory perception. Trends Neurosci. *26*, 243–247.

Wilson, D.A., and Sullivan, R.M. (2003). Sensory physiology of central olfactory pathways. In Handbook of Olfaction and Gustation, R.L. Doty, ed. (New York: Marcel Dekker), pp. 181–201.

Winston, J.S., Henson, R.N., Fine-Goulden, M.R., and Dolan, R.J. (2004). fMRI-adaptation reveals dissociable neural representations of identity and expression in face perception. J. Neurophysiol. *92*, 1830–1839.

Wise, P.M., Olsson, M.J., and Cain, W.S. (2000). Quantification of odor quality. Chem. Senses *25*, 429–443.

Worsley, K.J., Marrett, S., Neelin, P., Vandal, A.C., Friston, K.J., and Evans, A.C. (1996). A unified statistical approach for determining significant voxels in images of cerebral activation. Hum. Brain Mapp. *4*, 58–73.

Xu, F., Liu, N., Kida, I., Rothman, D.L., Hyder, F., and Shepherd, G.M. (2003). Odor maps of aldehydes and esters revealed by functional MRI in the glomerular layer of the mouse olfactory bulb. Proc. Natl. Acad. Sci. USA *100*, 11029–11034.

Zhao, H., Ivic, L., Otaki, J.M., Hashimoto, M., Mikoshiba, K., and Firestein, S. (1998). Functional expression of a mammalian odorant receptor. Science *279*, 237–242.

Zou, Z., Horowitz, L.F., Montmayeur, J.P., Snapper, S., and Buck, L.B. (2001). Genetic tracing reveals a stereotyped sensory map in the olfactory cortex. Nature *414*, 173–179.

Zou, Z., Li, F., and Buck, L.B. (2005). Odor maps in the olfactory cortex. Proc. Natl. Acad. Sci. USA *102*, 7724–7729.

Zwaardemaker, H. (1895). Die Physiologie des Geruchs (Leipzig: Engelmann).